Dual mode supply system for DD coils

Manuele Bertoluzzo*, Giuseppe Buja, *Life Fellow, IEEE*, and Hemant Dashora
Department of Industrial Engineering, University of Padova, Padova, Italy
*Corresponding author: manuele.bertoluzzo@unipd.it

***Abstract* – DD coils are often selected as case study for the research activity about the dynamic wireless charging systems for electric vehicles and are proposed to setup the track and/or the pickup onboard the vehicles. Indeed, they offer good coupling performance, but their capability can be fully exploited only if both the track coil and the pickup have the same DD topology, otherwise the transferred power decreases substantially. This paper proposes to use a three-legs inverter to separately supply the two sub coils that form a DD coil. Adopting a suitable control strategy of the inverter, the dynamic wireless charging system is made able to perform an effective power transfer both to DD coil pickups and to spiral coil pickups. Condition under which this result is achieved and the required modifications of the supply system and of the coils are studied in the paper. The proposed solution is validated by means of simulations.**

Index Terms— dynamic wireless charging; DD coil; spiral coil; three-legs inverter.

I. INTRODUCTION

Coupled coils are the heart of the dynamic wireless charging (DWC) system and hence their arrangement is subject of active research activity both from the point of view of coil windings, cores [1], shields [2] and compensation networks [3]. Among the solutions proposed in the literature for the windings, that one designed as double D (DD) is widely used for both the track coils and the pickup. After their development [4], the DD coils have been enhanced in order to fulfill different requirements such as the decoupling of their constituting sub-coil [5], [6], or the lengthening of the space interval during which each track coil is coupled with the pickup [7]. The advantage offered by the DD coils is a high coupling coefficient; however, it is exploited only when both the track coil and the pickup are of DD type; indeed, when a pickup made of a rectangular spiral coil is coupled with a DD coil, the voltage induced across its terminals results sensibly lower that that obtained from a DD pickup, and, even more, when the spiral pickup is perfectly aligned with the track coil the induced voltage, and, hence, the transferred power, is zero [8]. In order to guarantee the interoperability of the track with both the pickups based on DD coils or on spiral coils, a different arrangement, based on a solenoidal geometry, has been proposed for the track coils [1].

The coils are usually connected to compensation networks (CN) that, depending on the particular application, are designed to fulfill different requirement; the main being the reduction of the sizing power of the inverter and the increase of the power transfer effectiveness and efficiency [9], [10].

This paper presents a solution to the interoperability problem based on the idea of maintaining the general DD geometry for the track coils, but making accessible the common point of their sub coils to supply them independently using a three-legs inverter. Two different supply modes are envisaged, one designed to transfer power to a DD pickup, and the other tailored for the pickups constitute by a rectangular spiral coil. The topic of designing the compensation network (CN) connected to the track coils is also considered, recognizing a class of CNs whose performance are not affected by the switching between the two supply modes.

The paper is organized as follows: Section II reviews briefly the structure and the functioning of the DD coils and of the relevant supply inverter and gives a qualitative description of the coupling characteristics of the pair made of two DD coils and of the pair made of one DD coil and one spiral coil. Section III describes the dual mode supply (DMS) and the conditions that make feasible its implementation; moreover, it details the control algorithms of the supply inverter in the two supply modes, the design of the compensation networks connected to the track coils, and the design of the coils themselves. Section IV verifies by simulation the performance of the proposed DMS considering the two kinds of coil pairs. Section V concludes the paper.

II. CONVENTIONAL DD COILS ARRANGMENT

A DD coil is formed by two equal coplanar sub coils, laid side by side, connected in series, and wound in opposite directions. The classical solution to supply the track DD coils of DWC systems is a single-phase inverter based on an H-bridge. Between the supply inverter and the DD coil is usually inserted a CN designed to implement some form of resonance that forces the currents flowing in the coils to be nearly sinusoidal; as a consequence, the voltages across the coils and the induced voltages are nearly sinusoidal as well.

The coupling between the two sub coils of a track DD coil and a pickup can be represented as in Fig. 1. In the figure, and in the following discussion, the electrical quantities involved in the system operations are considered sinusoidal and are represented by phasors. From the schematic, the expressions of the voltages existing across the terminals of each sub coil are readily obtained in the form

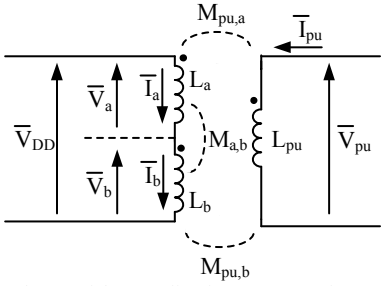

Fig. 1. Circuital scheme of the coupling between a track DD coil and the pickup.

$$\begin{cases}\bar{V}_a = j\omega L_a \bar{I}_a + j\omega M_{b,a}\bar{I}_b + j\omega M_{pu,a}\bar{I}_{pu} \\ \bar{V}_b = j\omega M_{a,b}\bar{I}_a + j\omega L_b \bar{I}_b + j\omega M_{pu,b}\bar{I}_{pu}\end{cases} \quad (1)$$

where L_a and L_b are the self-inductances of the sub coils a and b, $M_{a,b}$=$M_{b,a}$ is the mutual inductance between the two sub coils, and $M_{pu,a}$ and $M_{pu,b}$ are the mutual inductances between the pickup and each of the two sub coils. Being the two sub coils connected in series, it is $\bar{I}_a = \bar{I}_b$ and (1) can be rewritten as

$$\begin{cases}\bar{V}_a = j\omega\left(L_a + M_{b,a}\right)\bar{I}_a + j\omega M_{pu,a}\bar{I}_{pu} \\ \bar{V}_b = j\omega\left(L_b + M_{a,b}\right)\bar{I}_b + j\omega M_{pu,b}\bar{I}_{pu}\end{cases} \quad (2)$$

while the total voltage across the track coil terminals is

$$\bar{V}_{DD} = j\omega\left(L_a + L_b + 2M_{a,b}\right)\bar{I}_a + j\omega\left(M_{pu,a} + M_{pu,b}\right)\bar{I}_{pu} \quad (3)$$

and the voltage induced across the pickup terminals results

$$\bar{V}_{pu,ind} = j\omega\left(M_{pu,a} + M_{pu,b}\right)\bar{I}_a \quad (4)$$

The mutual inductances $M_{pu,a}$ and $M_{pu,b}$ depend on the relative position between the pickup and the track coil and on the orientation they have with respect to their relative motion direction. If the track coils and the pickup are oriented as in Fig. 2a, with the common side of the sub coils, which defines the y axis, orthogonal the motion direction, $M_{pu,a}$ and $M_{pu,b}$ have the qualitative profile reported with the dashed lines in the upper half of Fig. 3. In the figure, obtained considering a track and a pickup coil with the same dimensions and with no lateral misalignment, the mutual inductances are normalized with respect to their own maximum value and are plotted as a function of the pickup distance d with respect to the position perfectly aligned over the track coil. The distance has been normalized with respect to the sub coil dimension xDim, measured along the motion direction. From (4), the absolute value of the sum of the two mutual inductances is proportional to the magnitude $V_{pu,ind}$ of the voltage $\bar{V}_{pu,ind}$ induced across the pickup; it has been normalized with respect to its maximum value and plotted in the same graph with the solid line. The pickup results to some extent faced to the track coil for a space interval spanning twice xDim and consequently the induced voltage is different from zero for a space interval about two time longer than xDim in both the directions, even if two points exists, denoted as null power points, where the induced voltage is zero even if the pickup still partially overlaps the track coil [8].

If the track coils and the pickup are oriented as in Fig. 2b, with the common side of the sub coils parallel to the motion

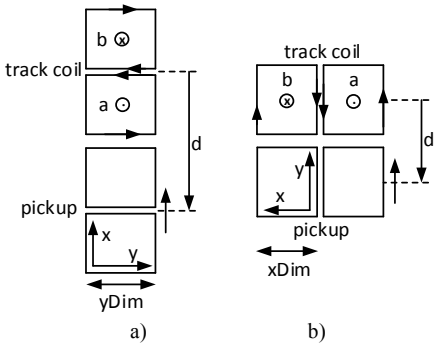

Fig. 2. Simplified representation of a track DD coil with two different orientations.

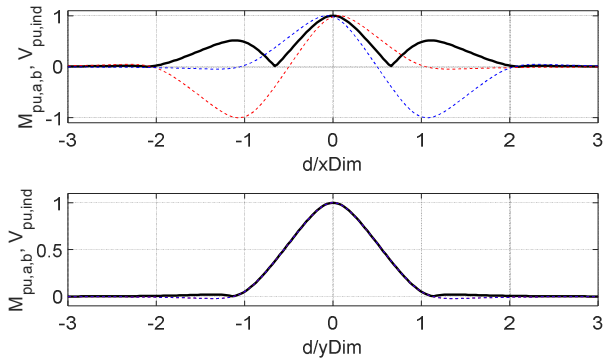

Fig. 3. Normalized $M_{pu,a}$, $M_{pu,b}$ and $V_{pu,ind}$ of the coupling between two DD coils vs. normalized position along the x and y axis.

direction, the profile of $M_{pu,a}$ is equal to that of $M_{pu,b}$ and both of them are nearly the same of the profile of $V_{pu,ind}$, as plotted in the lower half of Fig. 3. In this case the induced voltage does not exhibit the null power points but the space interval where it maintains a comparatively high value spans only one time the sub coil dimension yDim in both the directions.

If the pickup is a rectangular spiral coil with the same outer dimensions of the DD pickup and moves along the x axis, like in Fig. 2a, the mutual inductances and the induced voltage take the profiles sketched in the upper half of Fig. 4; here the plotted quantities have been normalized with respect to the maximum values taken by their counterparts when the DD pickup has been considered. Induced voltage is still considerable for a rather long space interval, but its maximum value is only about half of that reached coupling two DD coils and, moreover, it has a null power point when the pickup is aligned with the track coil. If the pickup moves parallel to the y axis, the induced voltage is always zero because $M_{pu,a}$=-$M_{pu,b}$, as sketched in the lower half of Fig. 4. From the above considerations it is clear that a track coil with DD topology, independently from the orientation of the coils, is not suited to supply energy to a spiral pickup.

III. THE DUAL MODE SUPPLY

The DMS is based on the idea of making the DWC system capable of switching between two supply mode: the DD-mode, described in the previous Section, enabled when the pickup is a DD coil, and the R-mode, developed to comply with the coupling characteristics of a rectangular spiral coil.

The R-mode is based on shifting the phase of the current flowing in one of the track sub coils by π, so that $\bar{I}_b = -\bar{I}_a$.

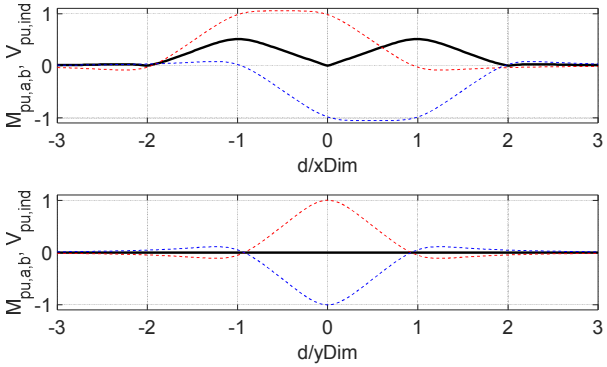

Fig. 4. Normalized $M_{pu,a}$, $M_{pu,b}$ and $V_{pu,ind}$ of the coupling between a DD coil and a rectangular spiral coil vs. normalized position along the x and y axis.

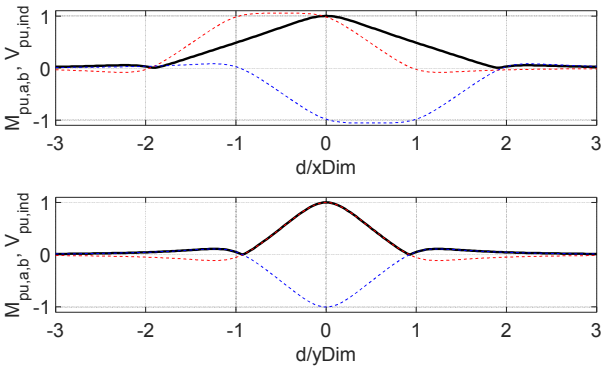

Fig. 5. Normalized $M_{pu,a}$, $M_{pu,b}$ and $V_{pu,ind}$ of the coupling between a DD coil supplied in R-mode and a rectangular spiral coil vs. normalized position along the x and y axis.

Consequently, the voltages across the track sub coils changes from (2) into

$$\begin{cases} \bar{V}_a = j\omega\left(L_a - M_{b,a}\right)\bar{I}_a + j\omega M_{pu,a}\bar{I}_{pu} \\ \bar{V}_b = j\omega\left(L_b - M_{a,b}\right)\bar{I}_b + j\omega M_{pu,b}\bar{I}_{pu} \end{cases} \quad (5)$$

and (4) becomes

$$\bar{V}_{pu,ind} = j\omega\left(M_{pu,a} - M_{pu,b}\right)\bar{I}_a \quad (6)$$

The profiles of the normalized $V_{pu,ind}$ obtained from (6) and considering the pickup moving along the x or y axis are plotted with the solid lines in Fig 5; in both cases they are higher than those shown in Fig. 4, thus demonstrating that the R-mode enables the power transfer from a track DD coil to a rectangular spiral pickup.

Implementing the capability of switching from the DD-mode to the R-mode according to the pickup topology requires to set up the transmitting side of the DWC system according to the architecture shown in Fig. 6. The track is set up using modified DD coils formed by two independent sub coils, each one endowed with its own CN, and supplied by a three-legs inverter. Beside the change in the coils arrangement, the DWC system must fulfill some requirements and limitations about the supply inverter control strategy, the topology of the compensation networks CN_a and CN_b, and the geometry of the sub coil in order to transfer effectively power to both the kinds of pickup.

A. Supply inverter

Switching between the DD-mode and the R-mode is performed changing the strategy for the generation of the gate signals of the inverter power switches.

In DD-mode, both the switches of the leg LGc, where the terminal C of the CNs is connected, are kept opened while those of LGa and LGb, where terminals A and B are connected, are

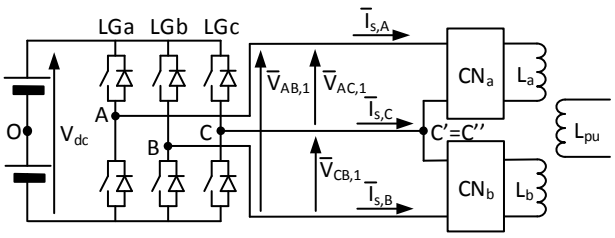

Fig. 6. Connection of the three-phase inverter to the DD coil.

commanded with 50% duty cycle. The amplitude $V_{AB,1}$ of the first harmonic of the inverter output voltage can be regulated adjusting the dc-side voltage or using the phase shift technique. In the first case, the switches of LGa are commanded in phase opposition to those of LGb so that V_{AB} is a square wave having first harmonic amplitude equal to [11]

$$V_{AB,1} = \frac{4}{\pi}V_{dc} \quad (7)$$

Instead, the phase shift technique provides for a constant V_{dc}, maintains the 50% duty cycle for the gate signals of LGa and LGb but imposes an adjustable phase shift Ø between them. This technique gives rise to a voltage $v_{AB}(t)$ with a three-level waveform and a first harmonic amplitude given by

$$V_{AB,1} = V_{DC}\frac{4}{\pi}sin\left(\frac{\emptyset}{2}\right) \quad (8)$$

The DD-mode supply is equivalent to connecting CN_a and CN_b in series, so that, if the same impedance is seen at their terminals, only half of $V_{AB,1}$ is applied to each CN.

The R-mode supply is based on the phase shift technique and uses the gate signal of the upper switch of LGc as phase reference for the the commands of LGa and LGb. If they are synchronous, the first harmonic components $\bar{V}_{AC,1}$ and $\bar{V}_{CB,1}$ of the voltages applied across the CNs terminals are in phase opposition and have equal amplitude $V_{AC,1}$ and $V_{CB,1}$ given by expressions similar to (8). In this case, the full available voltage is applied to each CN and higher current is expected to flow in the sub coils for a given value of Ø.

It is also possible to impose two different phase shift angles $\emptyset_a$ and $\emptyset_b$ to supply CN_a and CN_b with voltages having first harmonic components with different amplitudes, in this case, however, they are no more in phase opposition because their phase relation results a function of the difference between $\emptyset_a$ and $\emptyset_b$, as exemplified in Fig. 7. In the upper half of the figure the voltages of terminals A, B and C with respect to the middle point O of the dc bus are plotted after a normalization with respect to $V_{dc/2}$. The three voltages have equal amplitude, but $v_{AO}(t)$ and $v_{BO}(t)$ have been a bit reduced in the figure for ease of comparison. In the lower half, the corresponding voltages $v_{AC}(t)$ and $v_{CB}(t)$ and their relevant first harmonic components $v_{AC,1}(t)$ and $v_{CB,1}(t)$ are plotted with the solid and the dashed lines, respectively. From the figure it is easily found that $v_{AC,1}(t)$ lags the first harmonic of $v_{CO}(t)$ of $(\pi+\emptyset_a)/2$ while $v_{CB,1}(t)$ leads it of $(\pi-\emptyset_b)/2$. Consequently, being the phase shift between $v_{AC,1}(t)$

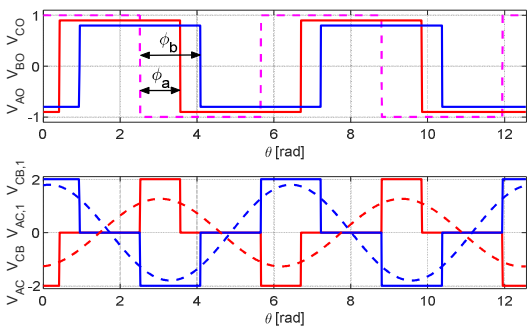

Fig. 7. Phase and phase-to-phase voltages of the supply inverter.

and $v_{CB,1}(t)$ equal to $\pi+(\emptyset_a-\emptyset_b)/2$, the two voltages are in phase opposition only if $\emptyset_a=\emptyset_b$.

B. Compensation networks

Most of the CNs used in the track of DWC systems have topologies derived from the general scheme of Fig. 8a [7], hereafter designed as the "reference" CN. The components of the reference CN are considered purely reactive and are denoted by their reactances X_s, X_p and X_t; X_C is the reactance of the coil and the impedance Z_{ref} accounts for the voltage induced by the pickup. In this paper it is supposed that the design requirements of the DWC system do not rely on particular values of the CN reactances, but are satisfied fixing the ratios k_s, k_p and k_t of X_s, X_p, and X_t to X_C. Following this approach, different compensation techniques are implemented assigning properly k_s, k_p, and k_t; for example, if k_s=-1, k_p=∞, and k_t=0, the series compensation is implemented; if k_s=1, k_p=-1, and k_t=0, the LCL CN is obtained; if k_s=1-n, k_p=n-1, and k_t=-n, with 0<n<1, the LCC compensation is set up [12].

In the case of a conventional DD coil, X_C is derived from the first term of (3) in the form

$$X_C = \omega\left(L_a + L_b + 2M_{a,b}\right) \tag{9}$$

while the reflected impedance $Z_{ref,a,b}$ is expressed by

$$\dot{Z}_{ref} = \frac{\omega^2\left(M_{pu,a}+M_{pu,b}\right)^2}{\dot{Z}_{pu}} \tag{10}$$

worked out analyzing the circuit of Fig. 1 and using (3) and (4) and denoting with $\dot{Z}_{pu}$ the impedance given by the pickup reactance and by the CN and the load connected to the pickup.

1) Equivalent CN in DD-mode supply

For the implementation of the dual mode supply the common point C of the sub coils a and b must be accessible to external connections. According to this requirement, with simple circuital manipulations, the scheme of Fig. 8a is redrawn as in Fig. 8b, where the two sub coils are represented and the reactance of each component of the CN is split into two equal contributes.

From (2), the reactances of the two sub coils are

$$\begin{cases} X_{SC,a,DD} = \omega\left(L_a + M_{a,b}\right) \\ X_{SC,b,DD} = \omega\left(L_b + M_{a,b}\right) \end{cases} \tag{11}$$

while the reflected impedances $\dot{Z}_{ref,a,DD}$ and $\dot{Z}_{ref,b,DD}$, each accounting for the voltages induced by $\bar{I}_{pu}$ across the corresponding sub coil, are given by

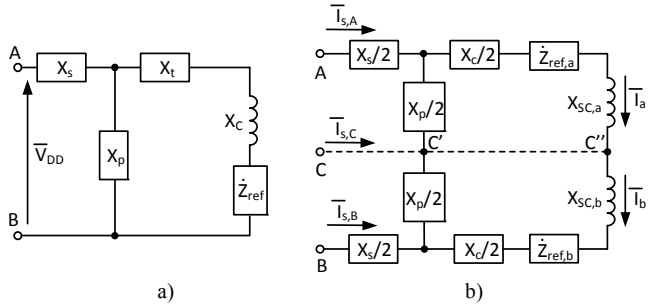

a) b)

Fig. 8. Connection of a single-phase inverter to a conventional DD track coil in the DD-mode supply (a) and its equivalent circuit (b).

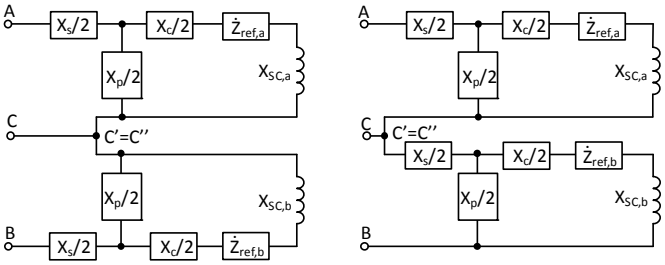

a) b)

Fig. 9. Connection of the three-phase inverter to a modified DD coil in the R-mode supply

$$\begin{cases} \dot{Z}_{ref,a,DD} = \frac{\omega^2 M_{pu,a}\left(M_{pu,a}+M_{pu,b}\right)}{\dot{Z}_{pu}} \\ \dot{Z}_{ref,b,D} = \frac{\omega^2 M_{pu,b}\left(M_{pu,a}+M_{pu,b}\right)}{\dot{Z}_{pu}} \end{cases} \tag{12}$$

If L_a=L_b and $\dot{Z}_{ref,a,DD} = \dot{Z}_{ref,b,DD} = \dot{Z}_{ref}/2$, points C' and C'' have the same potential and can be connected together and to the terminal C, as shown in Fig. 9a, without causing any variation in the functioning of the circuit. In particular, being C left open in the DD-mode supply, $\bar{I}_a$ is maintained equal to $\bar{I}_b$.

The condition L_a=L_b is fulfilled building two equal sub coil, instead, the condition $\dot{Z}_{ref,a,DD} = \dot{Z}_{ref,b,DD} = \dot{Z}_{ref}/2$ requires that $M_{pu,a}$=$M_{pu,b}$; by Fig. 3, it happens when a DD coil pickup moves along the y axis.

The scheme of Fig. 9a is perfectly correspondent to the circuital topology sketched in Fig. 6. This correspondence demonstrates that it is possible to setup two separate sub coils and the relevant CNs according to the scheme in Fig. 9a so that when the three-legs inverter operates in DD-mode, i.e. the terminal C is open, they jointly behave as a conventional DD coil supplied by a single-phase inverter through the reference CN.

2) Equivalent CN in R-mode supply

When the circuit of Fig. 9a is supplied in R-mode, voltages are impressed to the three terminals A, B, and C of the CNs to reverse the phase of the current $\bar{I}_b$ so that $\bar{I}_a = -\bar{I}_b$. In this condition, from (5), the reactances of the sub-coils are

$$\begin{cases} X_{SC,a,R} = \omega\left(L_a - M_{a,b}\right) \\ X_{SC,b,R} = \omega\left(L_b - M_{a,b}\right) \end{cases} \tag{13}$$

while the reflected impedances, considering that $\bar{I}_b$ is in phase opposition with respect to its DD-mode counterpart, changes into

$$\begin{cases} \dot{Z}_{ref,a,R} = \frac{\omega^2 M_{pu,a}\left(M_{pu,a}-M_{pu,b}\right)}{\dot{Z}_{pu}} \\ \dot{Z}_{ref,b,R} = \frac{-\omega^2 M_{pu,b}\left(M_{pu,a}-M_{pu,b}\right)}{\dot{Z}_{pu}} \end{cases} \tag{14}$$

The circuit in Fig. 9a can be redrawn as in Fig. 9b. Comparison of the latter one with Fig. 8a shows that in R-mode each sub coil behaves as it was connected to a CN having the same topology of the reference CN but formed by components with halved reactances. Because of this difference, neither CNa nor CNb has the same electrical behavior of the reference CN; however, if $X_{SC,a,R}$=$X_{SC,b,R}$=$X_C/2$ and $\dot{Z}_{ref,a,R} = \dot{Z}_{ref,b,R} =$

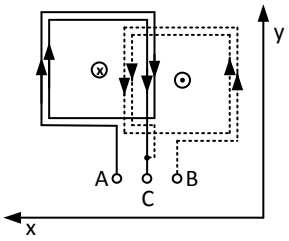

Fig. 10. Simplified representation of a bipolar pad.

$\dot{Z}_{ref}/2$, the ratios k_s, k_p, and k_c relevant to CN_a and CN_b result equal to those of the reference CN. Consequently, when R-mode is enabled, each sub coil with the relevant CN satisfies the same design requirements of the reference CN.

Comparison of (11) and (13) shows that the condition $X_{SC,a,R}=X_{SC,b,R}=X_C/2$ is achieved only if $M_{a,b}=0$, i.e. if there is no coupling between the two sub coils; the condition $\dot{Z}_{ref,a,R} = \dot{Z}_{ref,b,R} = \dot{Z}_{ref}/2$, by (14), requires that $M_{pu,a}$=-$M_{pu,b}$. By Fig. 5, the latter condition is satisfied when a rectangular spiral pickup moves along the y axis.

C. Track coil

All the condition derived in the previous Subsection about the track coil are satisfied by the sub coil that form a DD coil except for the requirement of having $M_{a,b}=0$.

A coil arrangement with this property is described in [5], [6] where an evolution of the DD coils, denoted as bipolar pad, is presented. The bipolar pads are formed by two sub coils connected in series; the sub coils are equal, thus assuring that $L_a=L_b$ and, as sketched in Fig. 10, are overlapped as much as necessary to have $M_{a,b}=0$. The profiles of $M_{pu,a}$ and $M_{pu,b}$ of a bipolar pad are a little different from those relevant to a DD coil, but thanks to the symmetry of the bipolar pads with respect to the y axis, they satisfy the condition $M_{pu,a}=M_{pu,b}$ when the pickup is a DD coil and the condition $M_{pu,a}$=-$M_{pu,b}$, when the pickup is a rectangular spiral coil. Implementation of the DMS requires that the sub coils common point is made accessible to be connected to the terminal C.

IV. Simulation Results

The functioning of the DMS has been tested by simulations performed in the Matlab/Simulink environment. The case study DWC system has the parameters reported in Tab. I and the mutual inductances follow he profiles of Figs. 3 and 5. The load connected to the pickup in an electric vehicle is constituted by a rectifier followed by a dc/dc converter that supplies the battery and the traction drive; in the simulations it has been represented by an equivalent resistance. A reference resonant CN with LCL

Tab. I: DD-coils parameters

Parameter	Symbol	Value
Sub-coil x dimension	xDim	0.4 m
Sub coil y dimension	yDim	0.4 m
Sub coil inductances	L_a, L_b	31 µH
Maximum mutual inductances	$M_{pu,a,max}$, $M_{pu,b,max}$	4.5 µH
Supply angular frequency	ω	2π·85000 rad/s
Dc bus voltage	V_{dc}	450 V
Equivalent load supplied by the pickup	R_L	2.1 Ω

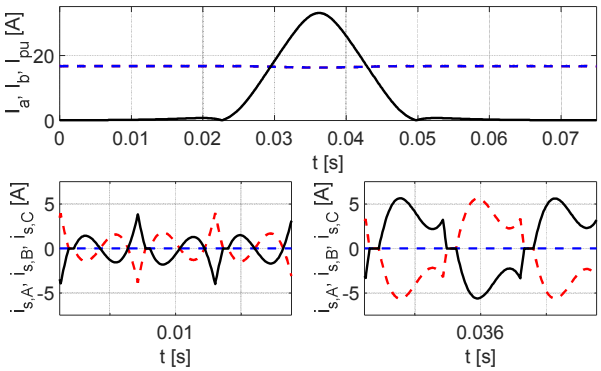

Fig. 11. Sub coils and pickup currents (top) and supply inverter phase currents (bottom) in DD-mode.

topology has been designed for the track coil while a series resonant compensation is used for the pickup. The variations of L_a and L_b as a function of the pickup position, originated by the presence of ferrite cores, have been neglected.

The first test considered a track coil coupled to a DD coil pickup moving along the y axis; as demonstrated in the previous Sections, the latter condition is necessary to have both the supply modes performing correctly. The supply inverter operates in DD-mode with phase shift $\emptyset=\pi$ while the mutual inductances $M_{pu,a}$ and $M_{pu,b}$ increases up to the maximum and then decreases back near to zero. Profiles of the magnitudes I_a, I_b and I_{pu} of the current phasors $\bar{I}_a$, $\bar{I}_b$ and $\bar{I}_{pu}$ are reported in the upper half of Fig 11as a function of the time; the first two are plotted using the dashed line while the third is denoted by the solid line. As expected, I_a and I_b are equal and, because of the functioning of the LCL CNs, are nearly constant and independent from the variation of the reflected load. The profile of I_{pu}, instead, reflects the variations of the coupling coefficients and reaches its maximum when the pickup is aligned with the track coil. The supply inverter instantaneous phase currents are plotted in the lower half of Fig. 11; $i_{s,A}(t)$ is denoted by the solid line, $i_{s,B}(t)$ and $i_{s,C}(t)$ by the dashed ones. As LGb is open, $i_{s,C}(t)$ is equal to zero while $i_{s,A}(t)$=-$i_{s,B}(t)$. The latter ones have the typical waveforms found when LCL CNs are used: if the transferred power is low, as it happens around t=0.01s, when the track coil and the pickup are poorly coupled, they are highly distorted and have small first harmonic components. If the transferred power increases, the currents waveforms are less distorted because their first harmonic components become considerable, as it happens at t=0.036 s, when the coupling is maximum. The amplitude V_L of the voltage

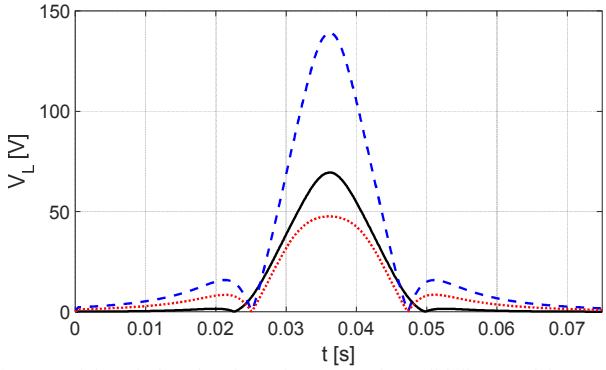

Fig. 12. Pickup induced voltage in DD-mode (solid line) and in R-mode (dashed line).

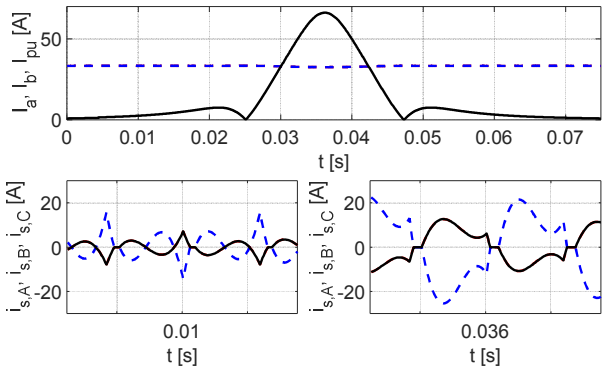

Fig. 13. Sub coils and pickup currents (top) and supply inverter phase currents (bottom) in R-mode with $\emptyset_a=\emptyset_b=\pi$.

applied across R_L is reported with the black solid line in Fig. 12; because of the resonant series compensation, apart from the voltage drop across the series resistance of the pickup, it is equal to $V_{pu,ind}$ and indeed it follows faithfully the profile plotted in the lower half of Fig. 3.

In the second simulation the coupling with a spiral rectangular coil is studied enabling the R-supply mode. The same test described above has been repeated using the mutual inductance profiles of Fig. 5 obtaining the current profiles of Fig. 13; I_a and I_b follow two equal and nearly constant profiles. The CNs are now supplied by twice the voltage of DD-mode, and the current magnitudes have two times the value obtained in the first simulation. The magnitude I_{pu} have the expected profile reported in Fig. 5. The inverter phase currents $i_{s,A}(t)$ and $i_{s,B}(t)$ are equal to each other while $i_{s,C}(t)$ is equal to the opposite of their sum; apart from the higher amplitude, the waveforms of the three currents are similar to those plotted in Fig. 11, thus confirming that switching from DD-mode to R-mode maintains the same functioning of the reference CN. Because of the higher currents in the track sub coils, the maximum value of V_L is two times that obtained in DD-mode, as shown by the blue dashed line in Fig. 12.

A third simulation have been performed maintaining the R-mode and setting $\emptyset_a=\emptyset_b=\pi/3$ to halve the voltage applied to the CNs and operate in the same conditions of DD-mode. Magnitudes and instantaneous values of the currents are reported in Fig. 14. The profiles of I_a and I_b result much more sensitive to the variation of the reflected load and this effect reflects on I_{pu} and in voltage applied to the load, plotted with the red dotted line in Fig. 12, which is lower than expected. The supply currents

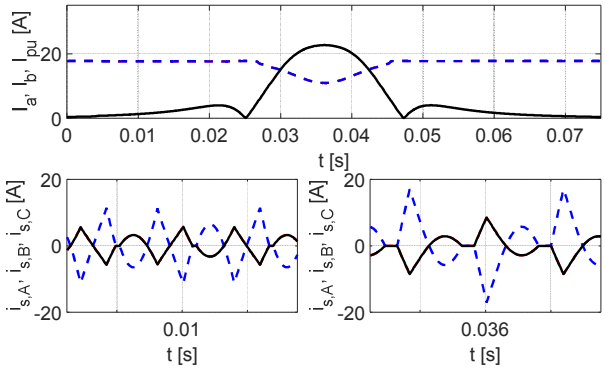

Fig. 14. Sub coils and pickup currents (top) and supply inverter phase currents (bottom) in R-mode with $\emptyset_a=\emptyset_b=\pi/3$.

amplitude is actually reduced, but their waveforms differ from those plotted in Fig. 13 because the supply voltage in not a square wave. The discrepancy with respect to the expected behavior can be ascribed to the effect of the dead time; in the simulations it has been set at 1μs, which represent about 12.5% of the active period of the supply voltage with the given phase shift.

V. Conclusions

The paper proposed to supply independently the two sub-coils of a DD track coil to implement two different supply modes, suitable for DD coil pickups and rectangular spiral coil pickups, in order to effectively transfer power to electric vehicles irrespectively from the arrangement of the onboard coils. This approach requires to use a three-legs supply inverter controlled with the phase shift technique and to design the track coils in such a way to nullify the mutual inductance between their sub coils. The validity of the proposal has been checked by simulations obtaining results in agreement with those derived theoretically.

References

[1] W.J. Li, J.H. Lu, G.R. Zhu, W. Zhang, and J. Jiang, "Design and research of a double-sided flux coupler in inductive power transfer system," proc. of annual conference of the IEEE Industrial Electronics Society, Florence, 2016, pp. 6033-6037.

[2] P. Alotto, M. Guarnieri, and F. Moro, "A Boundary integral formulation on unstructured dual grids for eddy-current analysis in thin shields," IEEE Transactions on Magnetics, vol. 43, n° 4 , pp. 1173-1176, 2007.

[3] W. Zhang and C.C. Mi, "Compensation topologies of high-power wireless power transfer systems," in *IEEE Transactions on Vehicular Technology*, vol. 65, no. 6, pp. 4768-4778, June 2016.

[4] M. Budhia, J.T. Boys, G.A. Covic, and C.-Y. Huang, Member, "Development of a single-sided flux magnetic coupler for electric vehicle IPT charging systems," *IEEE Transactions on Industrial Electronics*, vol. 60. no. 1, pp. 318-328, 2013.

[5] G.A. Covic, M.L.G. Kissin, D. Kacprzak, N. Clausen, and H. Hao, "A bipolar primary pad topology for EV stationary charging and highway power by inductive coupling," in Procs. of IEEE Energy Conversion Congress and Exposition, pp.1832-1838, 2011

[6] A. Zaheer, H. Hao, G.A. Covic, and D. Kacprzak, "Investigation of multiple decoupled coil primary pad topologies in lumped IPT systems for interoperable electric vehicle charging," in *IEEE Transactions on Power Electronics*, vol. 30, no. 4, pp. 1937-1955, April 2015.

[7] M. Bertoluzzo, G. Buja, and H.K. Dashora, "Design of DWC system track with unequal DD coil set," IEEE Transactions on Transportation Electrification, vol. 3, n° 2, pp. 380-391, 2017.

[8] M. Bertoluzzo, G. Buja, and H. Dashora, "Avoiding null power point in DD coils", in Procs. of IEEE PELS Workshop on Emerging Technologies: Wireless Power (WoW), 2019.

[9] M. Bertoluzzo, R. Jha, and G. Buja, "Power transfer profile boosting in DWC systems by two-element compensation network," in Procs. of IEEE PELS Workshop on Emerging Technologies: Wireless Power (WoW), 2019.

[10] Y. H. Sohn, B. H. Choi, E. S. Lee, G. C. Lim, G. H. Cho, and C. T. Rim, "General unified analyses of two-capacitor inductive power transfer systems: equivalence of current-source SS and SP compensations," *IEEE Trans. on Power Electron.*, vol. 30, no. 11, pp. 6030-6045, Nov. 2015.

[11] M.H. Rashid, "Power electronics circuits, devices, and applications," Third edition, Pearson/Prentice-Hall publications 2004, chap. 6.

[12] B. Li, J.-H. Lu, W.-J. Li, G.-R. Zhu, "Realization of CC and CV mode in IPT system based on the switching of doublesided LCC and LCC-S compensation network," in Procs. of Int. Conf. on Industrial Informatics - Computing Technology, Intelligent Technology, Industrial Information Integration (ICIICII), pp. 364 – 367, 2016.